Cell

Senataxin Associates with Replication Forks to Protect Fork Integrity across RNA-Polymerase-II-Transcribed Genes

Amaya Alzu,[1,4] Rodrigo Bermejo,[1,4,5] Martina Begnis,[1,6] Chiara Lucca,[1] Daniele Piccini,[1] Walter Carotenuto,[1] Marco Saponaro,[1,7] Alessandra Brambati,[1,2] Andrea Cocito,[1] Marco Foiani,[1,3] and Giordano Liberi[1,2,*]
[1]The FIRC Institute of Molecular Oncology (IFOM) Foundation, Via Adamello 16, 20139 Milan, Italy
[2]Istituto di Genetica Molecolare del Consiglio Nazionale delle Ricerche (IGM-CNR), Via Abbiategrasso 207, 27100 Pavia, Italy
[3]DSBB-Università degli Studi di Milano, Via Celoria 26, 20139 Milan, Italy
[4]These authors contributed equally to this work
[5]Present address: Instituto de Biología Funcional y Genómica, CSIC/USAL, Calle Zacarías González 2, 37007 Salamanca, Spain
[6]Present address: Cancer Research UK, London Research Institute, 44 Lincoln's Inn Fields, London WC2A 3PX, UK
[7]Present address: Clare Hall Laboratories, Cancer Research UK, London Research Institute, Blanche Lane, South Mimms EN6 3LD, UK
*Correspondence: giordano.liberi@igm.cnr.it
http://dx.doi.org/10.1016/j.cell.2012.09.041

SUMMARY

Transcription hinders replication fork progression and stability. The ATR checkpoint and specialized DNA helicases assist DNA synthesis across transcription units to protect genome integrity. Combining genomic and genetic approaches together with the analysis of replication intermediates, we searched for factors coordinating replication with transcription. We show that the Sen1/Senataxin DNA/RNA helicase associates with forks, promoting their progression across RNA polymerase II (RNAPII)-transcribed genes. *sen1* mutants accumulate aberrant DNA structures and DNA-RNA hybrids while forks clash head-on with RNAPII transcription units. These replication defects correlate with hyper-recombination and checkpoint activation in *sen1* mutants. The Sen1 function at the forks is separable from its role in RNA processing. Our data, besides unmasking a key role for Senataxin in coordinating replication with transcription, provide a framework for understanding the pathological mechanisms caused by Senataxin deficiencies and leading to the severe neurodegenerative diseases ataxia with oculomotor apraxia type 2 and amyotrophic lateral sclerosis 4.

INTRODUCTION

Replication forks slow down when encountering DNA secondary structures, DNA lesions, and DNA-bound proteins (Mirkin and Mirkin, 2007). Stalled forks are potentially genotoxic because they can be engaged by dangerous recombination activities (Branzei and Foiani, 2010). Transcription is the major physiological obstacle for replication (Aguilera, 2005; Bermejo et al., 2012; Rudolph et al., 2007), and failure to assist fork progression across transcription units leads to DNA damage (Bermejo et al., 2009, 2011; Brewer and Fangman, 1988; Huertas and Aguilera, 2003; Sabouri et al., 2012). Uncoordinated clashes between transcription and replication are likely a contributor to the replication stress (Bermejo et al., 2012), a hallmark of cancer (Bartkova et al., 2006; Di Micco et al., 2006).

In eukaryotes, both head-on and codirectional collisions between replication and transcription occur and hamper fork progression (Azvolinsky et al., 2009; Bermejo et al., 2009; Deshpande and Newlon, 1996). Members of the conserved family of Pif1 DNA helicases facilitate fork progression past protein-DNA barriers, including those at transcribed genes (Azvolinsky et al., 2009; Ivessa et al., 2003; Sabouri et al., 2012; Steinacher et al., 2012). The replication checkpoint contributes to prevent replication and transcription interference by disassembling the RNA polymerase (RNAP) III preinitiation complex (Clelland and Schultz, 2010) and by counteracting abnormal fork transitions at RNAPII-transcribed genes (Bermejo et al., 2011). RNAPII-transcribed genes are organized in chromatin loops (Hampsey et al., 2011), and the S phase architecture of messenger RNA (mRNA) genes depends on DNA topoisomerase II (Bermejo et al., 2009). The THO/TREX-2 complexes couple RNAPII transcription (Gómez-González et al., 2011) with mRNA export through the nuclear envelope, a process known as gene gating (Blobel, 1985). The ATR checkpoint phosphorylates key nucleoporins to counteract gene gating, thus neutralizing the topological tension generated when forks encounter gated genes (Bermejo et al., 2011).

Because DNA and RNA synthesis generate positive supercoiling downstream of moving DNA and RNA polymerases, head-on collisions between replisomes and RNAPs are expected to generate tremendous topological constraints (Olavarrieta et al., 2002; Wang, 2002). Negative supercoiling forms behind transcription bubbles, whereas replicated chromatids undergo precatenation (Wang, 2002). Unsolved topological constraints lead

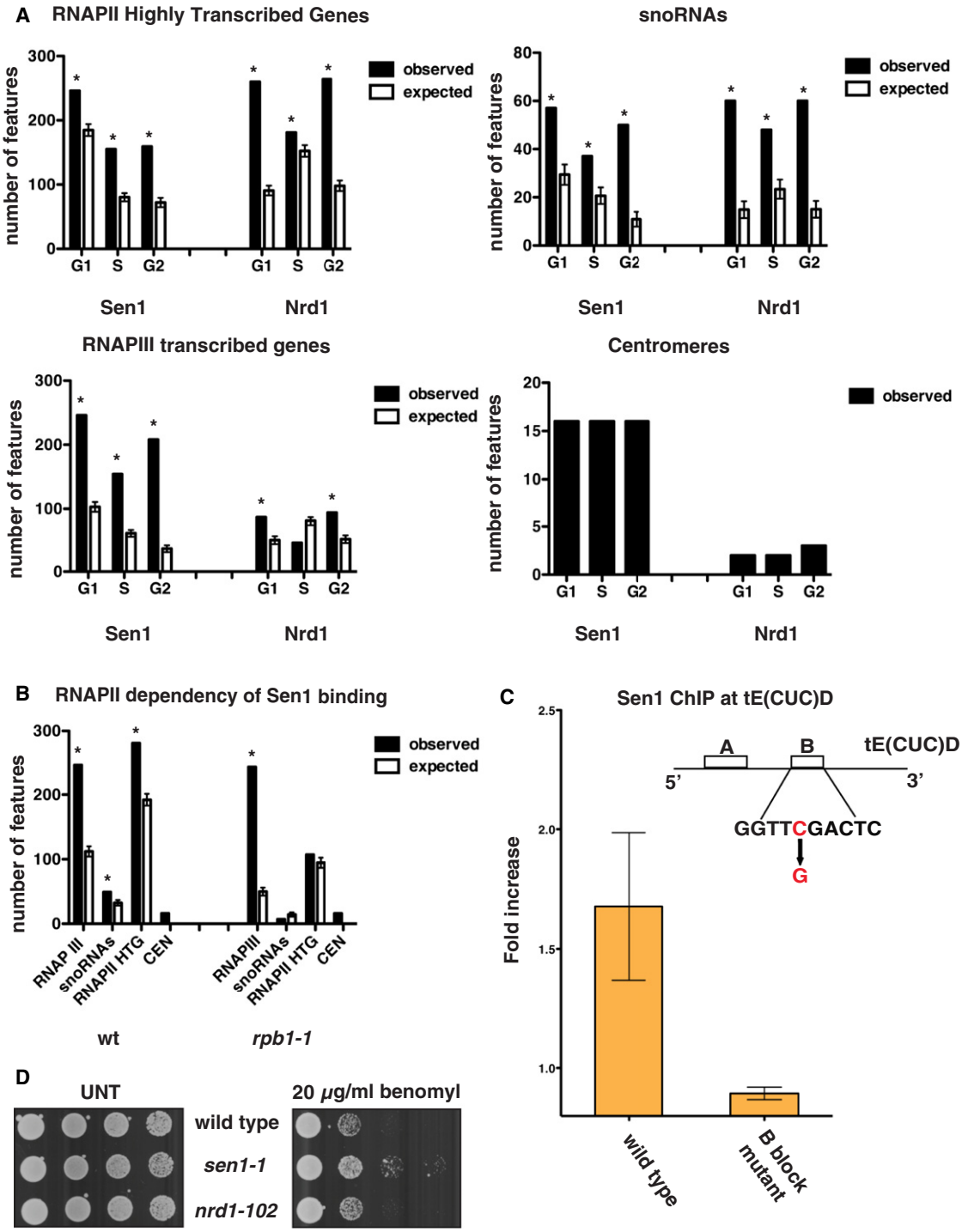

Figure 1. Genome-wide Analysis of Sen1 and Nrd1 Localization during the Cell Cycle

(A) *SEN1-* (Sen1) and *NRD1-FLAG* (Nrd1) strains were blocked in G1 phase by α-factor treatment (G1) and were released at 23°C in either 0.2 M HU for 60 min (S phase; S) or nocodazole for 180 min (G2/M). Samples were collected in each cell-cycle phase to analyze the genomic distribution of factors by ChIP-chip. The number of features bound by each factor in the ChIP experiments (observed) as well as in bioinformatic simulations is shown for highly transcribed RNAPII genes, snoRNAs, RNAPIII genes, and centromeres (see Experimental Procedures). Data represent the mean ±SD of three independent simulations (expected). Asterisks indicate features showing a statistically significant difference between observed and simulated binding. The statistical significance of Sen1 and Nrd1 binding to centromeres could not be calculated by this method due to the reduced total number—sixteen—of these elements.

(B) WT and *rpb1-1* cells were arrested in G2/M phase as in Figure 1A, transferred to 37°C for 1 hr to inactivate the RNAPII, and then processed for ChIP-chip to analyze Sen1 binding.

to the accumulation of dangerous recombinogenic DNA structures. Positive supercoiling can result in fork reversal (Postow et al., 2001), while R-loop formation depends on negative supercoiling accumulation (Drolet, 2006). Whereas in prokaryotes DNA-RNA hybrids can trigger replication (Kogoma, 1997; Pomerantz and O'Donnell, 2008), a growing body of evidence suggests that, in eukaryotes, the DNA-RNA hybrids at R-loops promote chromosomal rearrangements (Gan et al., 2011; Gómez-González et al., 2011; Gottipati et al., 2008; Helmrich et al., 2011; Huertas and Aguilera, 2003; Li and Manley, 2005; Mischo et al., 2011; Paulsen et al., 2009; Tuduri et al., 2009; Wahba et al., 2011). R-loop accumulation is enhanced in the absence of mRNA biogenesis factors (Paulsen et al., 2009; Stirling et al., 2012), including the THO/TREX-2 complexes (Domínguez-Sánchez et al., 2011; Huertas and Aguilera, 2003) and the SR protein SRSF1 (Li and Manley, 2005). These factors sequester nascent transcripts, thus preventing RNA reannealing to the template. Topoisomerase I (Drolet, 2006; Tuduri et al., 2009), RNase H (Wahba et al., 2011), and Senataxin (Sen1 in budding yeast) (Mischo et al., 2011; Skourti-Stathaki et al., 2011; Stirling et al., 2012) have been involved in suppressing R-loop accumulation.

The Senataxin gene encodes a conserved DNA/RNA helicase with multiple roles in RNA metabolism (Suraweera et al., 2009) and is found mutated in the two severe neurodegenerative disorders ataxia-ocular apraxia type 2 (AOA2) (Moreira et al., 2004) and amyotrophic lateral sclerosis type 4 (ALS4) (Chen et al., 2004). The best-characterized function of yeast Sen1 is to terminate RNAPII transcripts acting in a complex with two RNA-binding proteins, Nrd1 and Nab3. The Sen1-Nrd1-Nab3 complex terminates nonpolyadenylated RNA species that include small nuclear (sn) and small nucleolar (sno) RNAs (Steinmetz et al., 2001; Ursic et al., 1997), cryptic unstable transcripts (Arigo et al., 2006; Thiebaut et al., 2006), and aberrant mRNAs (Rondón et al., 2009). It has been proposed that, both in yeast and mammals, Senataxin/Sen1 removes R-loops that form physiologically during transcription termination (Mischo et al., 2011; Skourti-Stathaki et al., 2011) and whose pathological accumulation induces hyperrecombination (Mischo et al., 2011; Stirling et al., 2012).

We previously identified Sen1 as a physical interactor of the Srs2 recombination DNA helicase (Chiolo et al., 2005). In this study, we found that Sen1 assists DNA metabolic processes other than transcription termination. We show that a fraction of Sen1 associates with replication forks and protects the integrity of those forks that encounter highly expressed RNAPII genes. In the absence of Sen1, forks engaging RNAPII-transcribed genes in a head-on conformation accumulate aberrant DNA structures and DNA-RNA hybrids that likely prime unscheduled recombination events, checkpoint activation, and genome instability. Our data point to a role for Sen1 during chromosome replication in facilitating replisome progression across RNAPII-transcribed genes, thus preventing DNA-RNA hybrid accumulation when forks encounter nascent transcripts on the lagging strand template.

RESULTS

We investigated the genome-wide distribution of Sen1 and Nrd1 during the cell cycle by ChIP-chip. In G1-, S-, and G2/M-phase-arrested cells, Sen1 and Nrd1 were enriched at highly transcribed RNAPII genes and snoRNA and snRNA units (Figure 1A and Figure S1 available online). Sen1, and to a minor extent Nrd1, was also associated with RNAPIII-transcribed units and centromeres (Figures 1A and S1). Transcription-defective *rpb1-1* RNAPII mutants (Nonet et al., 1987) specifically prevented Sen1 recruitment at RNAPII-transcribed genes (Figures 1B and S1), and a point mutation in the B block promoter element of the intronless *tE(CUC)D* (tRNA) gene counteracted Sen1 association (Figure 1C). Thus, the presence of these RNA species influences Sen1 chromatin binding at transcribed genes. These data are consistent with a role for Sen1-Nrd1 in processing/terminating RNAPII (Creamer et al., 2011; Rasmussen and Culbertson, 1998; Steinmetz et al., 2001; Ursic et al., 1997; Vasiljeva and Buratowski, 2006) and RNAPIII transcripts (DeMarini et al., 1992; Jamonnak et al., 2011; Wlotzka et al., 2011).

Sen1 binding to centromeres was RNAPII independent (Figures 1B and S1). Intriguingly, *sen1* mutations caused resistance to benomyl treatment (Figure 1D) and affected spindle pole body and/or microtubule functions (Page and Snyder, 1992; Vizeacoumar et al., 2010). We conclude that Sen1 influences multiple aspects of DNA metabolism besides RNAPII-mediated transcription.

ChIP-chip analysis showed that, in hydroxyurea (HU)-treated cells, Sen1, but not Nrd1, clusters correlated with bromodeoxyuridine (BrdU)-incorporating regions (Figure 2). Ablation of the *ARS607* origin (Shirahige et al., 1993) prevented the local association of Sen1 (Figure S2A). Sen1 association to replicating chromatin was not influenced by the presence of mRNA species (Figure S2B) and was also observed in cells experiencing S phase under unperturbed conditions (data not shown). Thus, Sen1, independently of Nrd1, seems to associate with moving replication forks. We next examined whether Sen1 assists origin firing and/or fork progression. Wild-type (WT) and temperature-sensitive *sen1-1* strains bearing an aminoacidic substitution in the essential helicase domain (DeMarini et al., 1992) were released from G1 phase at 37°C in the presence of HU. The two strains showed a comparable pattern of origin firing by genome-wide analysis of BrdU incorporation and by two-dimensional gel electrophoresis (2D gel) analysis (Figures S3A and S3B), suggesting that origin firing does not depend on Sen1. However, BrdU incorporation was reduced in *sen1-1* compared to WT cells in the proximity of the highly expressed *PDC1-TRX1* genes (Figure S3C). This locus is heavily transcribed and is a natural replication-pausing element due to replication-transcription interference (Azvolinsky et al., 2009). We analyzed

(C) Sen1 binding to a WT or a B-block promoter mutant *tE(CUC)D* gene was evaluated by ChIP, followed by qPCR in G2/M-arrested cells. Data represent the mean ±SD of three independent experiments.
(D) Serial dilutions of WT, *sen1-1*, and *nrd1-102* cells plated in the presence or absence (UNT) of benomyl.
See also Figure S1.

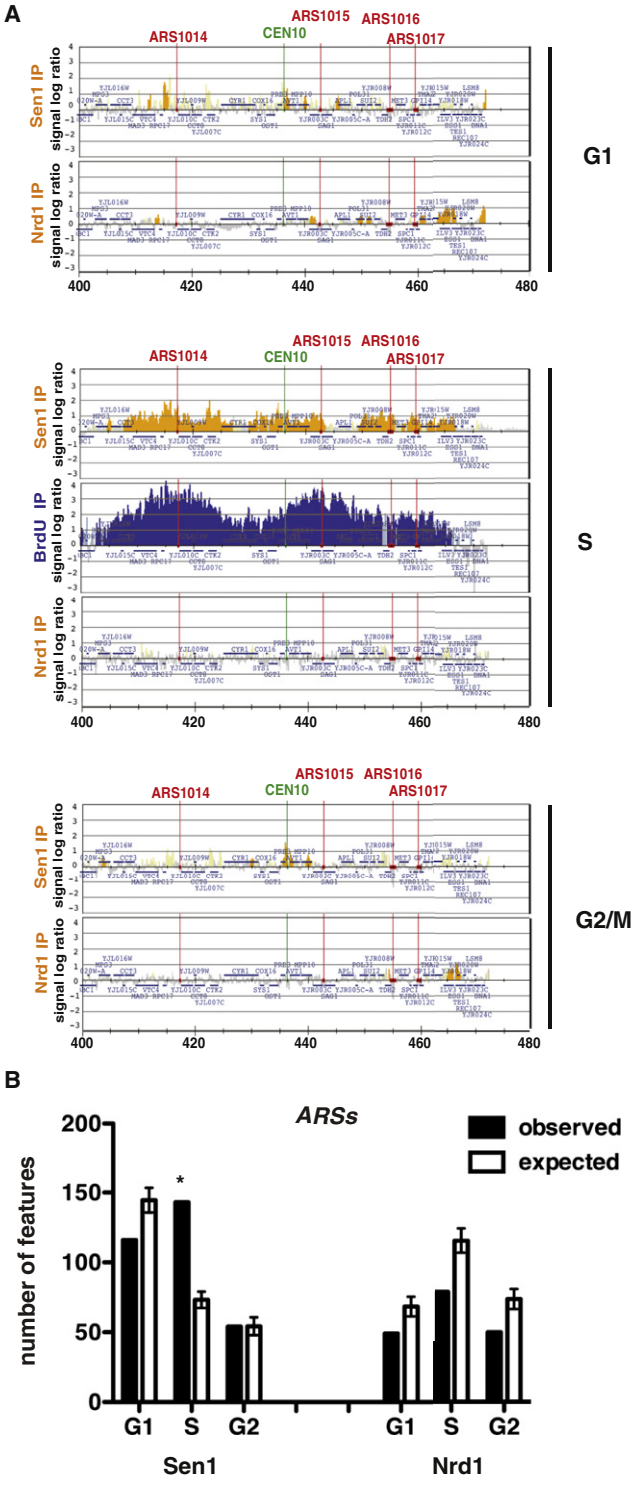

Figure 2. Sen1 Localizes at Replication Forks

(A) Sen1 and Nrd1 distributions at replication origins by ChIP-chip throughout the cell cycle. Cells were synchronized in G1, S, and G2/M phases, and Sen1 and Nrd1 binding profiles were obtained as in Figure 1A. Blue (BrdU-IP) histogram bars in the y axis show the average signal ratio in log2 scale on loci along the reported region on chromosome X in S-phase-arrested cells. Replication origin, ORF, and *CEN10* sequences are indicated.

(B) The number of features bound by each factor in the ChIP experiments (observed), as well as in bioinformatic simulations, is shown for *ARS* elements (see Experimental Procedures). Data represent the mean ±SD of three independent simulations (expected). Asterisks indicate features showing a statistically significant difference between observed and simulated binding. See also Figure S2.

the fate of replication intermediates at this specific location by 2D gel analysis in WT cells and in the conditional lethal strain *GAL::URL-HA-SEN1* in which Sen1 can be rapidly depleted in glucose medium (Figure 3). Cells were released from G1 into S phase, and samples were collected at different time points. We analyzed a 4,073 bp SphI fragment carrying the *PDC1-TRX1* genes and the *ARS1211* origin located at 315 bp from the right end of the fragment (Figure 3A). The most proximal active origins are located at 74 kb and 57 kb to the right and left ends, respectively. Hence, the 2D gel analysis monitors *ARS1211* left forks encountering head-on the *PDC1-TRX1* transcription units; the right forks instead immediately run off the restriction fragment, preventing the visualization of bubble-like intermediates. Accordingly, WT cells accumulated middle and large Y intermediates representing *ARS1211* left forks (Figure 3D). Discrete spots on the Y arc were also visible and likely resulted from fork-pausing events (Azvolinsky et al., 2009) (Figure 3D). Sen1-depleted cells exhibited accumulation of middle Y-shaped forks that persisted longer compared to WT cells, further confirming that Sen1 facilitates fork progression across the *PDC1-TRX1* region (Figure 3D). We carried out the same analysis in the presence of HU, which affects the viability of *sen1* mutants (Mischo et al., 2011), and we found that, whereas WT cells accumulated large Ys, in Sen1-depleted cells, again, they were barely detectable (Figure 3E). *sen1* cells accumulated aberrant structures migrating along a diagonal spike within a 1.2 Kb region located 991 bp on the left side of *ARS1211* and overlapping with a large portion of the *PDC1* 3′ end (Figures 3E and 4A). The mass of these intermediates ranged from 1,548 to 2,769 bps, spanning the entire 1.2 Kb region on the first dimension (Figure 4A). On the second dimension, they migrated faster than the middle Ys located within the same region. Hence, these abnormal molecules seem to accumulate at the expense of large Ys and may reflect a population of forks specifically slowing down within the *PDC1* C-terminal region (Figure 4A). Their fast migration on the second dimension may result from a Y-shaped structure containing partially replicated DNA at the fork-branching point. To test this hypothesis, we analyzed replication intermediates in *sen1* cells following treatment with Mung Bean single-strand nuclease on 2D gels. We found that the abnormal structures were sensitive to the nuclease treatment (Figure 4B), suggesting that, in *sen1* mutants, fork intermediates accumulate single-stranded DNA (ssDNA) gaps at the branching point in the proximity of the 3′ end of *PDC1*. The left forks arising from *ARS1211* encounter the *PDC1* transcript head-on, and the 3′ end of the mRNA molecule is annealed to the lagging strand template. It is possible that, in *sen1* mutants, *PDC1* DNA-RNA hybrids slow down incoming forks, generating unreplicated DNA (Figure 3A). ssDNA could also transiently accumulate at the nontranscribed strand (Figure 3A). We note that, because replication intermediates for 2D gel analysis were pretreated

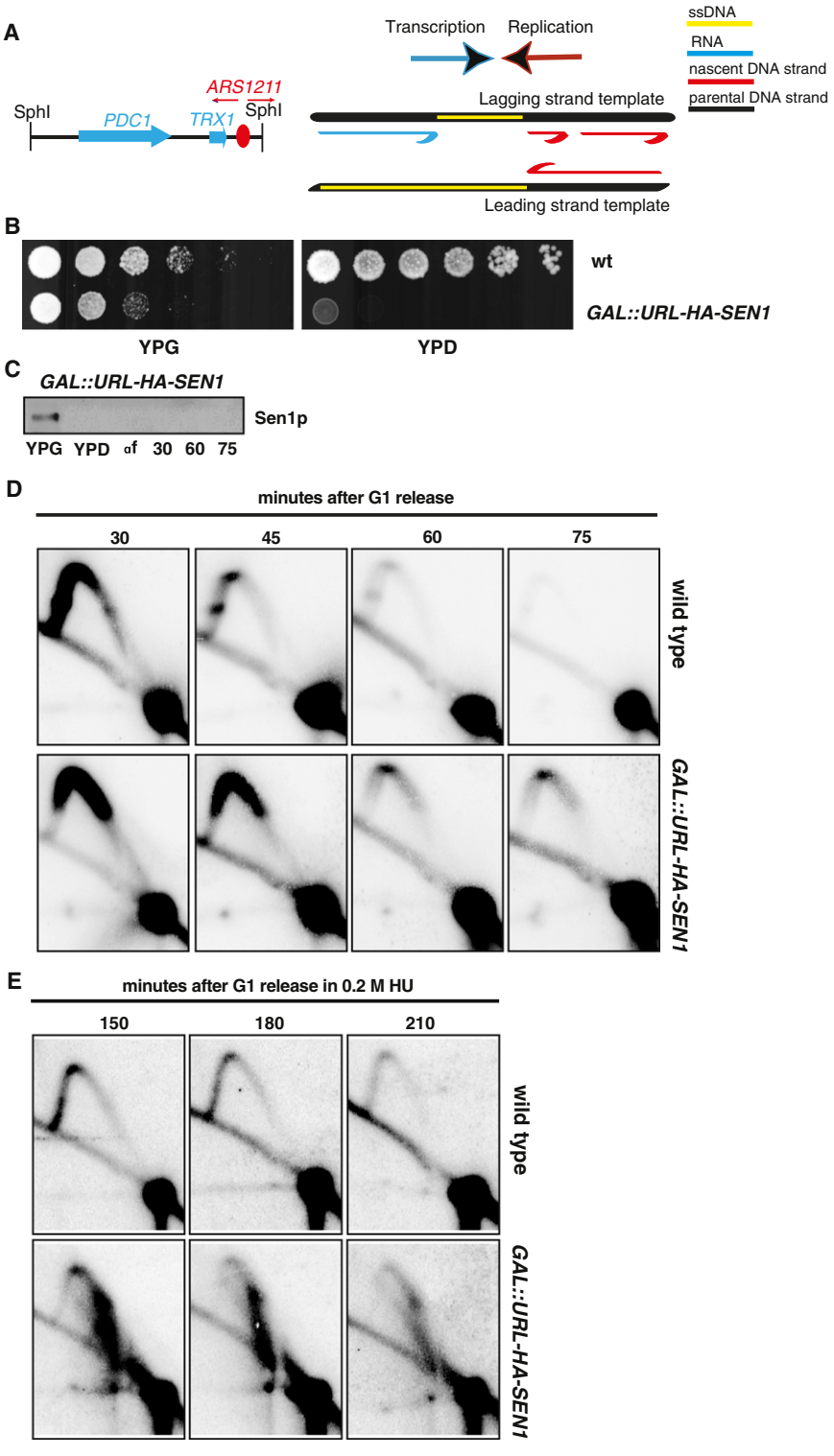

Figure 3. Sen1-Depleted Cells Exhibit Fork Defects at Highly Expressed RNAPII Genes *PDC1-TRX1*

(A) Schematic representation of 2D gel restriction strategy (left) and replication-transcription directionality at the *PDC1-TRX1* locus (right).

(B) Serial dilutions of WT and conditional lethal *GAL::URL-HA-SEN1* strains were spotted on glucose (YPD)- or galactose (YPG)-containing media.

(C–E) WT and *GAL::URL-HA-SEN1* cells were grown in YPG, transferred to YPD for 1 hr to switch off *SEN1*, presynchronized in G1, and released into cell cycle in YPD with or without 0.2 M HU. Cells were collected to assess Sen1 protein levels (C) and replication intermediates by 2D gel analysis in the absence (D) or presence of HU (E).

See also Figure S3.

with RNaseA or RNaseH (Figure 4B), gaps could also form at the lagging strand template where the RNA molecule was previously annealed. In any case, Sen1 should prevent the accumulation of DNA-RNA hybrids at the *PDC1* locus. We immunoprecipitated DNA-RNA hybrids in WT and Sen1-depleted cells by using the S9 antibody (Hu et al., 2006). The immunoprecipitated material was then amplified by quantitative PCR (qPCR) to specifically visualize hybrids at the *PDC1* locus. The experiments were carried out in WT and *GAL::URL-HA-SEN1* strains released from G1 phase into HU. In our experimental conditions, Sen1 was rapidly depleted in glucose-containing medium and, already in α-factor-arrested cells, was no longer detectable by western blot (Figure 3C). The *PDC1* transcript levels increased in G1-S in presence of HU about 2-fold (data not shown). WT and *sen1* cells in G1 exhibited a similar and very low level of hybrids (Figure 4C). WT cells in HU exhibited a transient and slight accumulation of hybrids that peaked at 150–180 min (Figure 4C). In contrast, in *sen1* mutants, hybrids dramatically accumulated and persisted at late time points (Figure 4C). We confirmed this observation also in an unperturbed S phase and at different transcribed loci (data not shown). We then used ChIP-qPCR with antibodies against Rfa1 to visualize the presence of Rfa-ssDNA nucleofilaments at the *PDC1* locus. WT cells exhibited very low levels of Rfa1-bound chromatin in G1 and in S phase. In Sen1-depleted cells, Rfa1 accumulated already in G1 and peaked in S phase at 180 min (Figure 4D). We conclude that Sen1 depletion causes accumulation of DNA-RNA hybrids and ssDNA regions in S phase. However, although the hybrids persisted, the Rfa-ssDNA nucleofilaments decreased at later time points.

We performed a 2D gel analysis on three additional loci in which forks encounter head-on RNAPII-transcribed units

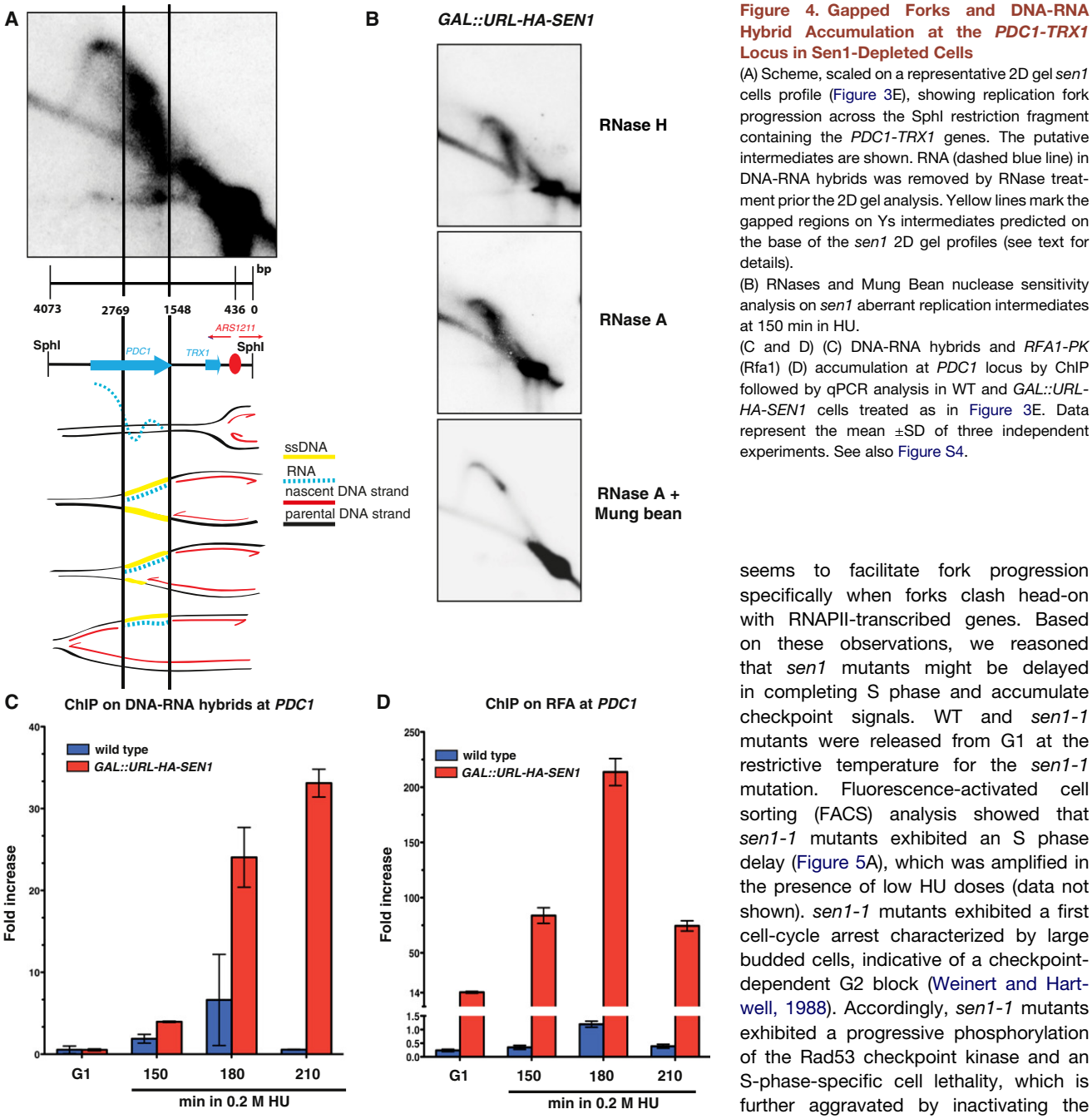

Figure 4. Gapped Forks and DNA-RNA Hybrid Accumulation at the *PDC1-TRX1* Locus in Sen1-Depleted Cells

(A) Scheme, scaled on a representative 2D gel *sen1* cells profile (Figure 3E), showing replication fork progression across the SphI restriction fragment containing the *PDC1-TRX1* genes. The putative intermediates are shown. RNA (dashed blue line) in DNA-RNA hybrids was removed by RNase treatment prior the 2D gel analysis. Yellow lines mark the gapped regions on Ys intermediates predicted on the base of the *sen1* 2D gel profiles (see text for details).

(B) RNases and Mung Bean nuclease sensitivity analysis on *sen1* aberrant replication intermediates at 150 min in HU.

(C and D) (C) DNA-RNA hybrids and *RFA1-PK* (Rfa1) (D) accumulation at *PDC1* locus by ChIP followed by qPCR analysis in WT and *GAL::URL-HA-SEN1* cells treated as in Figure 3E. Data represent the mean ±SD of three independent experiments. See also Figure S4.

(*SNR13-TRS31*, *SOD2-ERG11*, and *HYP2*). Again, Sen1 assisted fork progression across these regions, preventing pausing (Figures S4 and S5), although we did not detect massive accumulation of aberrant structures as in the case of the highly expressed *PDC1* locus. WT and Sen1-depleted cells exhibited comparable 2D gel profiles at regions in which forks encounter either RNAPII-transcribed genes codirectionally (*FBA1*, *PGK1*, *SSA4*, and *RPS13*) or RNAPIII-transcribed genes head-on (*tE(CUC)D*) (Figure S4 and data not shown). Thus, Sen1, consistent with being a 5′ to 3′ RNA/DNA helicase (Kim et al., 1999), seems to facilitate fork progression specifically when forks clash head-on with RNAPII-transcribed genes. Based on these observations, we reasoned that *sen1* mutants might be delayed in completing S phase and accumulate checkpoint signals. WT and *sen1-1* mutants were released from G1 at the restrictive temperature for the *sen1-1* mutation. Fluorescence-activated cell sorting (FACS) analysis showed that *sen1-1* mutants exhibited an S phase delay (Figure 5A), which was amplified in the presence of low HU doses (data not shown). *sen1-1* mutants exhibited a first cell-cycle arrest characterized by large budded cells, indicative of a checkpoint-dependent G2 block (Weinert and Hartwell, 1988). Accordingly, *sen1-1* mutants exhibited a progressive phosphorylation of the Rad53 checkpoint kinase and an S-phase-specific cell lethality, which is further aggravated by inactivating the *RAD9* checkpoint gene (Figures 5B–5D). These data suggest that *sen1-1* cells are impaired in S phase progression and accumulate ssDNA checkpoint signals at replication forks.

Notably, *nrd1-102* heat-sensitive mutants, carrying an amminoacidic substitution within the essential RNA recognition motif of Nrd1 (Conrad et al., 2000), treated at 37°C, did not exhibit replication fork pausing at RNAPII-transcribed genes (Figure S5 and data not shown), replicated DNA with a kinetic similar to WT cells, did not activate the Rad53 checkpoint, and failed to arrest in the first cell cycle (Figure 5). Moreover, the viability of *nrd1-102* mutants was not dependent on the presence of a functional

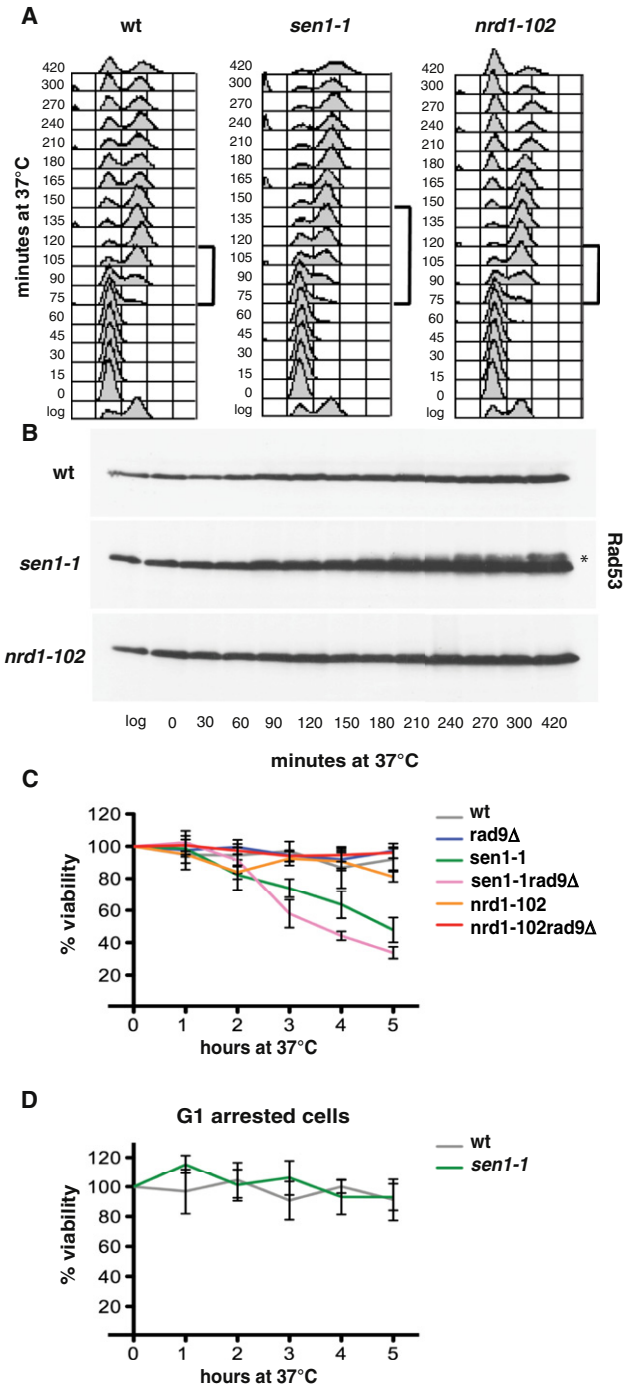

Figure 5. Replication Defects and DNA Damage Checkpoint Activation in *sen1* Mutants

(A–D) WT, *sen1-1*, and *nrd1-102* cells were released from G1 phase arrest into the cell cycle at 37°C. At the indicated time points, cell samples were processed for FACS analysis to measure the DNA content (A) or TCA protein precipitation to detect Rad53 protein (B). Brackets indicate the extent of S phase. Rad53 phosphorylated isoforms are indicated by an asterisk. Survival curves of the indicated yeast strains after release from G1 phase into cell cycle at 37°C (C) or blocked in G1 at 37°C (D). Data represent the mean ±SD of three independent experiments. See also Figure S5.

RAD9 gene (Figure 5C). These results suggest that, although Sen1 and Nrd1 both seem implicated in transcription termination, a fraction of Sen1 has additional roles in preventing fork instability across certain transcribed units and in suppressing DNA damage checkpoint activation.

We next examined whether replication fork arrest and checkpoint activation in *sen1* mutants correlate with genome instability. We found, in accordance with a recent study (Mischo et al., 2011), that *sen1-1* mutants were lethal in the absence of homologous recombination (HR) proteins, such as Rad51, Srs2, Mre11, and Sgs1 (Figure 6A). In addition, other factors that preserve the fork integrity, including the replisome components Ctf4 (Lengronne et al., 2006), Mrc1, and Tof1 (Katou et al., 2003) or Rtt109/Mms22 complex, which acts in the intra-S H3-K56 acetylation signaling pathway (Collins et al., 2007), were also essential for *sen1-1* viability (Figure 6A). In contrast, *nrd1-102* mutants did not require any of these factors for survival (Figure S6; see also Mischo et al., 2011). Moreover, although *sen1-1* mutants displayed reduced viability in combination with *rad51Δ* at the higher temperatures, *RAD51* deletion rescued the synthetic lethality of *sgs1Δ sen1-1* at 25°C and, partially, the one of *srs2Δ sen1-1* at 37°C (Figure 6B). Thus, HR is essential in *sen1-1* mutants, and further inactivation of the Sgs1 or Srs2 DNA helicases leads to the accumulation of lethal recombination intermediates. *sen1-1* mutants, but not *nrd1-102*, displayed a high rate of recombination between direct repeats with a preference for genomic deletion events (Figure 6C). Moreover, *sen1-1* mutants, but not *nrd1-102* mutants, exhibited a high frequency of chromosome loss (Figure 6D).

Taken together, our findings suggest that a fraction of Sen1 moves with replication forks and counteracts DNA-RNA hybrid formation at sites of collision between the replisome and RNAPII-transcribed genes. Sen1 role at forks is separable from its function in transcription termination and seems critical to prevent checkpoint activation and genome instability.

DISCUSSION

Transcription hinders fork progression, leading to recombination-mediated genome rearrangements (Aguilera, 2005; Bermejo et al., 2012; Rudolph et al., 2007 and references therein). Transcription can therefore cause replication stress (Bermejo et al., 2012) that is a hallmark of cancer (Bartkova et al., 2006; Di Micco et al., 2006) and of certain neurodegenerative disorders (Yurov et al., 2011 and references therein).

In bacteria, which have single origins of replication, the topological complexity caused by transcription-replication interference is alleviated by their typical genomic organization characterized by codirectionality between forks and transcription (Rocha, 2008). Nevertheless, multiple DNA/RNA helicases cooperate to coordinate replication-transcription collisions (Boubakri et al., 2010). In eukaryotes, because chromosome replication is mediated by multiple origins, transcription-replication clashes often occur in a head-on mode, thus increasing the topological complexity. Moreover, RNAPII genes are widely dispersed within the eukaryotic genome and undergo cotranscriptional events, such as mRNA export (Köhler and Hurt, 2007), which impose significant topological constraints (Bermejo et al., 2012; Koster

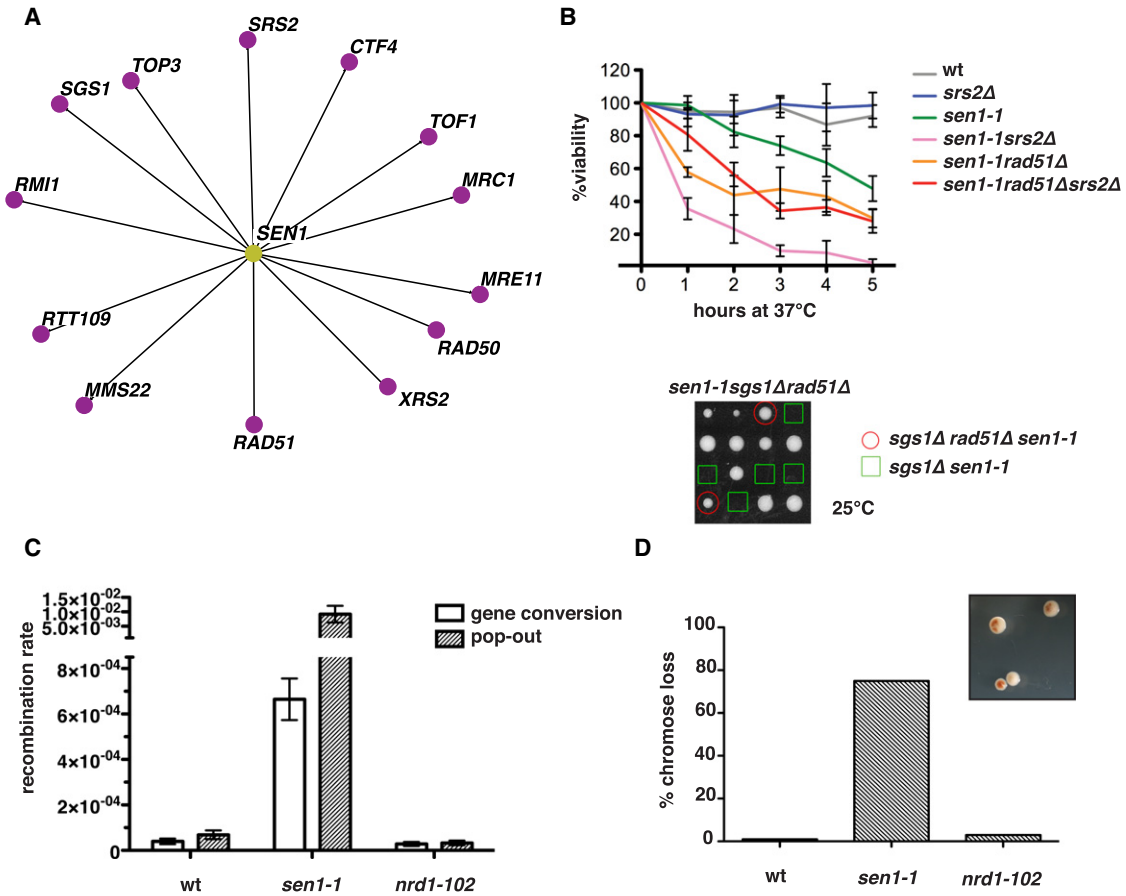

Figure 6. Replication/Recombination-Dependent Genotoxicity in *sen1-1* Mutants

(A–D) (A) *SEN1* synthetic lethality map generated by Osprey (B) survival curves of the indicated yeast strains after release from G1 phase into cell cycle at 37°C. Tetrads obtained from sporulation of diploids heterozygous for the indicated mutations were grown at 25°C. Gene conversion and pop-out rates (C) and chromosome loss frequency (D) were determined for WT, *sen1-1*, and *nrd1-102* strains at 30°C. Data in (B) and (C) represent the mean ±SD of three independent experiments. An example of red/white sector phenotype in *sen1-1* mutants is shown in (D). See also Figure S6.

et al., 2010). Recent observations indicate that the S phase architecture of RNAPII genes is highly regulated (Bermejo et al., 2009), and the ATR checkpoint counteracts gene gating to allow fork progression across RNAPII transcription units (Bermejo et al., 2011). However, it is unclear how the fork displaces the transcription apparatus once the gated transcription loop is released from the nuclear envelope (Bermejo et al., 2012).

Here, we show that the RNA/DNA helicase Senataxin counteracts DNA-RNA hybrids specifically when forks encounter RNAPII transcription units. Our data, together with the biochemical observation that Senataxin translocates with a 5′ to 3′ polarity, preferentially displacing DNA-RNA hybrids (Kim et al., 1999), suggest that Sen1 has a key role in coordinating head-on replication-transcription collisions.

The following observations point out a function for Senataxin within the chromosome replication process: (1) a fraction of Sen1 associates with moving forks; (2) in all the cases analyzed, Sen1 counteracts fork pausing at RNAPII-transcribed units clashing head-on with replication forks; (3) HU treatment induces fork instability at highly transcribed regions and cell lethality in *sen1* mutants; (4) DNA-RNA hybrids accumulate in S phase when Sen1 is ablated. Moreover, our findings that another population of Sen1 associates with Nrd1 and binds RNAPII and RNAPIII genomic elements throughout the cell cycle and that Nrd1 does not affect S phase events strongly suggest that Senataxin has evolved at least two functions—one in facilitating RNA biogenesis and one in assisting fork progression in head-on encounters with RNAPII-transcribed genes.

The current view suggests that the RNA-processing defects caused by Senataxin inactivation lead to the accumulation of R-loops that trigger genotoxic recombinogenic events (Mischo et al., 2011; Skourti-Stathaki et al., 2011). The R-loop structure resembles the D-loop structure of recombination intermediates and is characterized by the presence of a very stable DNA-RNA hybrid duplex on the transcribed strand and by a symmetric ssDNA region on the nontranscribed strand. R-loop formation seems facilitated by the accumulation of negative supercoiling behind the transcription bubble (Drolet, 2006), and its recombinogenic potential is due to the ssDNA. If the accumulation of

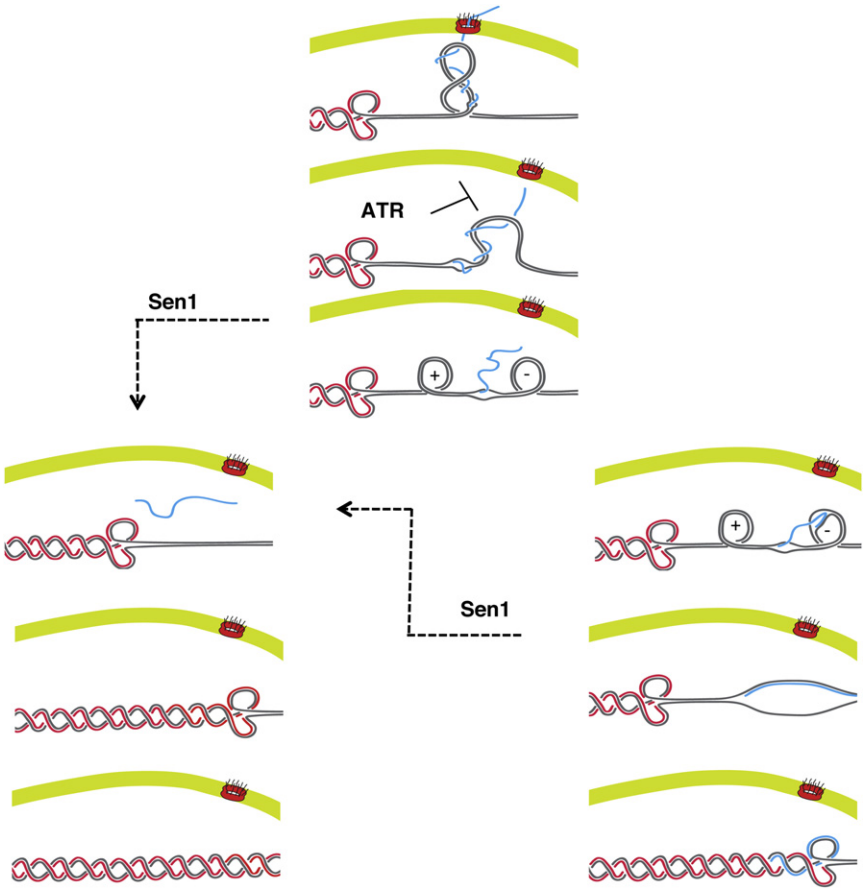

Figure 7. Model for DNA-RNA Hybrid Accumulation in *sen1* Mutants at Sites of Collision between Replication and Transcription

The ATR checkpoint inhibits gene gating to allow fork progression through topological barriers imposed by RNAPII-transcribed genes. Following gene loop dismantlement, twin-supercoiled domains transiently form, and nascent transcripts may anneal to the negatively supercoiled DNA behind the transcription bubble, leading to DNA-RNA hybrid formation. Sen1 moves with the fork, preventing DNA-RNA hybrid accumulation at those genomic regions at which transcription collides head-on with replication. In the absence of Sen1, DNA-RNA hybrids persist on the lagging strand template. Replication across the nontranscribed strand might be facilitated by the uncoupling of leading- and lagging-strand synthesis.

R-loops in Senataxin mutants is indeed caused by transcription termination problems, we would expect accumulation of DNA-RNA hybrids at the constitutively transcribed *PDC1* locus also in G1. Our data seem at odds with this scenario as we found that DNA-RNA hybrids significantly accumulate in *sen1* mutants in S phase, but not in G1 phase, and this defect correlates with the accumulation of aberrant DNA replication intermediates. The finding that Sen1-depleted G1 cells accumulate Rfa-ssDNA nucleofilaments but no RNA-DNA hybrids may in fact reflect a slow transcription mode owing to transcription termination problems. Based on our data, we propose that the replicative—and not the transcriptional—function of Sen1 counteracts DNA-RNA hybrids specifically in S phase at those locations at which transcription collides head-on with replication. The finding that DNA-RNA hybrids accumulate in S phase in *sen1* mutants implies that the DNA-RNA hybrid has to face an incoming fork. This raises the possibility that those forks arising from *ARS1211*, while approaching the 3′ end of the *PDC1* transcripts, transiently uncouple leading and lagging strand synthesis and replicate across the nontranscribed strands (Figure 7). Indeed, fork-uncoupling events have been described (Pagès and Fuchs, 2003). The scenario described above would suggest a multistep process for the accumulation of hybrids in *sen1* mutants. The triggering event for hybrid formation might be the topological constraints that arise when forks collide head-on with RNAPII-transcribed units right after the DNA damage-response-mediated dismantling of gene gating (Bermejo et al., 2012). The resolution of the transcribed loop might then generate the twin topological domain characterized by the positive and negative supercoiling ahead of or behind the transcription bubble, respectively (Figure 7) (Liu and Wang, 1987). The residual abortive mRNAs, particularly at highly transcribed genes, might then anneal with the template within the underwound negatively supercoiled region (Drolet, 2006), thus leading to R-loop formation (Figure 7). A backtracking RNAPII might also contribute to hybrid formation (Nudler, 2012). In the absence of Sen1, fork passage would then replicate across the R-loop, leaving behind DNA-RNA hybrid regions (Figure 7). Replication across the R-loop would also correlate with the progressive reduction of Rfa-ssDNA nucleofilaments, as we observed. Whether RNase H activities process hybrids in *sen1* mutants remains to be elucidated.

Our observations indicate that DNA-RNA hybrids transiently accumulate also in WT cells going through S phase. These results suggest that, when transcription and replication collide head-on, Sen1 actively displaces the hybrids that form in a physiological context on transcribed strands.

We also suggest that the recombinogenic and genome instability events observed in the absence of a functional *sen1* are the result of faulty replication. In *sen1* mutants, the DNA damage checkpoint is proficient. In fact, *sen1* mutants generate checkpoint signals, likely due to fork pausing and/or DNA-RNA hybrid processing. Hence, it is expected that the ATR pathway is still functional in counteracting gene gating at transcribed units while forks approach.

In budding yeast, at least four fork-associated helicases (Azvolinsky et al., 2006; Cobb et al., 2003; Papouli et al., 2005) assist fork advancement, preventing unwanted recombination; Rmr3 displaces protein barriers, including those at RNAPIII

genes (Azvolinsky et al., 2006), while Sgs1 and Srs2 promote replication across trinucleotide repeats (Kerrest et al., 2009) and counteract hemicatenane accumulation (Liberi et al., 2005). We now show that Sen1 counteracts recombinogenic events when forks encounter RNAPII-transcribed units. Intriguingly, Sgs1 and Sen1 physically interact with Srs2 (Chiolo et al., 2005), and the corresponding mutants are synthetic lethal due to the accumulation of toxic Rad51 nucleofilaments that likely form at replication forks (Figure 6B; Gangloff et al., 2000).

AOA2 and ALS4 are both rare diseases caused by mutations in the Senataxin gene (Chen et al., 2004; Moreira et al., 2004). AOA2 cells are sensitive to DNA-damaging agents (Suraweera et al., 2007), although the molecular mechanisms causing these phenotypes are still unknown. Altogether, our data place Senataxin within a molecular network that preserves the integrity of replicating chromosomes and reinforce the notion that transcription represents a chronic stress for replication. We suggest that the failure to regulate the conflicts between replication and transcription in Senataxin-defective cells could contribute, in part, to the pathological features of AOA2 and ALS4.

EXPERIMENTAL PROCEDURES

Yeast Strains and Growth Conditions

Yeast strains used in this study are listed in Table S1 and are constructed as described in the Extended Experimental Procedures. Yeast strains were grown in YP media containing glucose at 2% w/v (YPD) or galactose at 2% w/v (YPG). α-factor was used at a final concentration of 2 μg/ml or, in the experiment shown in Figure 5D, 20 μg/ml. Nocodazole, benomyl, and HU drugs were used at a final concentration indicated in the figure legends. Details on growth conditions for individual experiments are described in the figure legends.

ChIP-chip, BrdU-IP Analysis, and Statistical Methods

S. cerevisiae oligonucleotide microarrays were provided by Affymetrix. The ChIP-chip and the BrdU-IP chip analysis were carried out and analyzed as described (Bermejo et al., 2011), employing anti-Flag monoclonal antibody M2 (Sigma-Aldrich, F1804) or anti-BrdU antibody (MBL, MI-11-3), respectively. A list of highly transcribed RNAPII genes has been obtained from the literature (Azvolinsky et al., 2009 and references therein). The list of RNAPIII genes includes all tRNAs, 5S rDNAs (*RND5-1-6*), *SNR6*, *RPR1*, *SCR1*, and *SNR52*. Evaluation of the significance of protein cluster distributions within the different genomic features was performed by confrontation to the model of the null hypothesis distribution generated by a Montecarlo-like simulation (Bermejo et al., 2009) (see also Extended Experimental Procedures).

qPCR ChIP Experiments

DNA-RNA hybrid precipitation was performed as previously described (Mischo et al., 2011), with some modifications (see Extended Experimental Procedures). Standard ChIP on Sen1, Rfa1, and Polα has been carried out by using the ChIP-chip protocol. ChIPed DNA levels were measured by quantitative real-time PCR by using the SYBR Green technique (SYBR Green PCR Master Mix, Applied Biosystems) and run in Roche Light Cycler 480 Real-Time PCR System. Sequences of the DNA primers are listed in Table S2. The results were analyzed by CT method as described in the Extended Experimental Procedures.

2D Gel Electrophoresis of Replication Intermediates

DNA replication intermediates were purified from in vivo psoralen crosslinked cells by using the CTAB methods and subjected to 2D gel electrophoresis as previously described (Liberi et al., 2006) (see also Extended Experimental Procedures). DNA samples, when indicated, were treated with 10 U Mung Bean (New England Biolabs) for 1 hr at 30°C or with 30 U RNaseH (Invitrogen) for 4 hr at 37°C before being subjected to 2D gel electrophoresis.

Genetic Methods and Other Techniques

Genetic analyses were performed by using standard procedures for mating, diploid selection, sporulation, and tetrad dissection. Survival of yeast strains at 37°C was evaluated as plating efficiency, and curves are the mean values from three independent experiments. For spot assays, yeast strains were grown at equal cellular concentrations and sequentially diluted 1:6 before being spotted onto plates with or without treatment. Intrachromosomal recombination rates were determined as previously described (Xu et al., 2004) by using yeast strains carrying a heteroallelic duplication of *LEU2*, with *URA3* between the *LEU2* genes. Chromosome loss was evaluated by a colony-sectoring assay previously described (Spencer et al., 1990). The frequencies of chromosome loss were calculated as percentage of red/white sectored colonies scored on plates containing minimal medium supplemented with 20–30 μg/ml of amino acids and 6 μg/ml of adenine. Flow cytometry cell-cycle analysis was performed on a Beckton Dickinson fluorescence-activated cell analyzer by using propidium iodide as DNA stain. For western blot analysis, protein extracts were prepared by TCA precipitation (Chiolo et al., 2005).

ACCESSION NUMBERS

The Gene Expression Omnibus database accession number for the experimental data reported in this paper is GSE39139.

SUPPLEMENTAL INFORMATION

Supplemental Information includes Extended Experimental Procedures, six figures, and two tables and can be found with this article online at http://dx.doi.org/10.1016/j.cell.2012.09.041.

ACKNOWLEDGMENTS

We thank Yuki Katou and Katsuhiko Shirahige for assistance with ChIP-chip map construction; Massimo Lopes, Ted Weinert, Michele Giannattasio, and all members of our labs for discussion; and Victor Gonzalez-Huici, Cheng-Fu Kao, Aurora Cerutti, Michael Culbertson, Rosella Visintin, Philip Hieter, and Hannah Klein for reagents, advice, and technical support. We also thank the Microarray Facility at the IFOM-IEO campus. A.B. is a student of the PhD program in Genetics, Molecular, and Cellular Biology of the University of Pavia. R.B. is supported by the Spanish Ministry of Science and Innovation (RYC-2010-07131 and BFU2011-24909) and the European Community's FP7 (under grant agreement 293770). This work was supported by grants from Associazione Italiana per la Ricerca sul Cancro (AIRC) and Telethon-Italy (GGP08057) to G.L.

Received: March 21, 2012
Revised: July 10, 2012
Accepted: September 20, 2012
Published: November 8, 2012

REFERENCES

Aguilera, A. (2005). mRNA processing and genomic instability. Nat. Struct. Mol. Biol. *12*, 737–738.

Arigo, J.T., Eyler, D.E., Carroll, K.L., and Corden, J.L. (2006). Termination of cryptic unstable transcripts is directed by yeast RNA-binding proteins Nrd1 and Nab3. Mol. Cell *23*, 841–851.

Azvolinsky, A., Dunaway, S., Torres, J.Z., Bessler, J.B., and Zakian, V.A. (2006). The S. cerevisiae Rrm3p DNA helicase moves with the replication fork and affects replication of all yeast chromosomes. Genes Dev. *20*, 3104–3116.

Azvolinsky, A., Giresi, P.G., Lieb, J.D., and Zakian, V.A. (2009). Highly transcribed RNA polymerase II genes are impediments to replication fork progression in Saccharomyces cerevisiae. Mol. Cell *34*, 722–734.

Bartkova, J., Rezaei, N., Liontos, M., Karakaidos, P., Kletsas, D., Issaeva, N., Vassiliou, L.V., Kolettas, E., Niforou, K., Zoumpourlis, V.C., et al. (2006).

Oncogene-induced senescence is part of the tumorigenesis barrier imposed by DNA damage checkpoints. Nature *444*, 633–637.

Bermejo, R., Capra, T., Gonzalez-Huici, V., Fachinetti, D., Cocito, A., Natoli, G., Katou, Y., Mori, H., Kurokawa, K., Shirahige, K., and Foiani, M. (2009). Genome-organizing factors Top2 and Hmo1 prevent chromosome fragility at sites of S phase transcription. Cell *138*, 870–884.

Bermejo, R., Capra, T., Jossen, R., Colosio, A., Frattini, C., Carotenuto, W., Cocito, A., Doksani, Y., Klein, H., Gómez-González, B., et al. (2011). The replication checkpoint protects fork stability by releasing transcribed genes from nuclear pores. Cell *146*, 233–246.

Bermejo, R., Lai, M.S., and Foiani, M. (2012). Preventing replication stress to maintain genome stability: resolving conflicts between replication and transcription. Mol. Cell *45*, 710–718.

Blobel, G. (1985). Gene gating: a hypothesis. Proc. Natl. Acad. Sci. USA *82*, 8527–8529.

Boubakri, H., de Septenville, A.L., Viguera, E., and Michel, B. (2010). The helicases DinG, Rep and UvrD cooperate to promote replication across transcription units in vivo. EMBO J. *29*, 145–157.

Branzei, D., and Foiani, M. (2010). Maintaining genome stability at the replication fork. Nat. Rev. Mol. Cell Biol. *11*, 208–219.

Brewer, B.J., and Fangman, W.L. (1988). A replication fork barrier at the 3′ end of yeast ribosomal RNA genes. Cell *55*, 637–643.

Chen, Y.Z., Bennett, C.L., Huynh, H.M., Blair, I.P., Puls, I., Irobi, J., Dierick, I., Abel, A., Kennerson, M.L., Rabin, B.A., et al. (2004). DNA/RNA helicase gene mutations in a form of juvenile amyotrophic lateral sclerosis (ALS4). Am. J. Hum. Genet. *74*, 1128–1135.

Chiolo, I., Carotenuto, W., Maffioletti, G., Petrini, J.H., Foiani, M., and Liberi, G. (2005). Srs2 and Sgs1 DNA helicases associate with Mre11 in different subcomplexes following checkpoint activation and CDK1-mediated Srs2 phosphorylation. Mol. Cell. Biol. *25*, 5738–5751.

Clelland, B.W., and Schultz, M.C. (2010). Genome stability control by checkpoint regulation of tRNA gene transcription. Transcription *1*, 115–125.

Cobb, J.A., Bjergbaek, L., Shimada, K., Frei, C., and Gasser, S.M. (2003). DNA polymerase stabilization at stalled replication forks requires Mec1 and the RecQ helicase Sgs1. EMBO J. *22*, 4325–4336.

Collins, S.R., Miller, K.M., Maas, N.L., Roguev, A., Fillingham, J., Chu, C.S., Schuldiner, M., Gebbia, M., Recht, J., Shales, M., et al. (2007). Functional dissection of protein complexes involved in yeast chromosome biology using a genetic interaction map. Nature *446*, 806–810.

Conrad, N.K., Wilson, S.M., Steinmetz, E.J., Patturajan, M., Brow, D.A., Swanson, M.S., and Corden, J.L. (2000). A yeast heterogeneous nuclear ribonucleoprotein complex associated with RNA polymerase II. Genetics *154*, 557–571.

Creamer, T.J., Darby, M.M., Jamonnak, N., Schaughency, P., Hao, H., Wheelan, S.J., and Corden, J.L. (2011). Transcriptome-wide binding sites for components of the Saccharomyces cerevisiae non-poly(A) termination pathway: Nrd1, Nab3, and Sen1. PLoS Genet. *7*, e1002329.

DeMarini, D.J., Winey, M., Ursic, D., Webb, F., and Culbertson, M.R. (1992). SEN1, a positive effector of tRNA-splicing endonuclease in Saccharomyces cerevisiae. Mol. Cell. Biol. *12*, 2154–2164.

Deshpande, A.M., and Newlon, C.S. (1996). DNA replication fork pause sites dependent on transcription. Science *272*, 1030–1033.

Di Micco, R., Fumagalli, M., Cicalese, A., Piccinin, S., Gasparini, P., Luise, C., Schurra, C., Garre', M., Nuciforo, P.G., Bensimon, A., et al. (2006). Oncogene-induced senescence is a DNA damage response triggered by DNA hyper-replication. Nature *444*, 638–642.

Domínguez-Sánchez, M.S., Barroso, S., Gómez-González, B., Luna, R., and Aguilera, A. (2011). Genome instability and transcription elongation impairment in human cells depleted of THO/TREX. PLoS Genet. *7*, e1002386.

Drolet, M. (2006). Growth inhibition mediated by excess negative supercoiling: the interplay between transcription elongation, R-loop formation and DNA topology. Mol. Microbiol. *59*, 723–730.

Gan, W., Guan, Z., Liu, J., Gui, T., Shen, K., Manley, J.L., and Li, X. (2011). R-loop-mediated genomic instability is caused by impairment of replication fork progression. Genes Dev. *25*, 2041–2056.

Gangloff, S., Soustelle, C., and Fabre, F. (2000). Homologous recombination is responsible for cell death in the absence of the Sgs1 and Srs2 helicases. Nat. Genet. *25*, 192–194.

Gómez-González, B., García-Rubio, M., Bermejo, R., Gaillard, H., Shirahige, K., Marín, A., Foiani, M., and Aguilera, A. (2011). Genome-wide function of THO/TREX in active genes prevents R-loop-dependent replication obstacles. EMBO J. *30*, 3106–3119.

Gottipati, P., Cassel, T.N., Savolainen, L., and Helleday, T. (2008). Transcription-associated recombination is dependent on replication in Mammalian cells. Mol. Cell. Biol. *28*, 154–164.

Hampsey, M., Singh, B.N., Ansari, A., Lainé, J.P., and Krishnamurthy, S. (2011). Control of eukaryotic gene expression: gene loops and transcriptional memory. Adv. Enzyme Regul. *51*, 118–125.

Helmrich, A., Ballarino, M., and Tora, L. (2011). Collisions between replication and transcription complexes cause common fragile site instability at the longest human genes. Mol. Cell *44*, 966–977.

Hu, Z., Zhang, A., Storz, G., Gottesman, S., and Leppla, S.H. (2006). An antibody-based microarray assay for small RNA detection. Nucleic Acids Res. *34*, e52.

Huertas, P., and Aguilera, A. (2003). Cotranscriptionally formed DNA:RNA hybrids mediate transcription elongation impairment and transcription-associated recombination. Mol. Cell *12*, 711–721.

Ivessa, A.S., Lenzmeier, B.A., Bessler, J.B., Goudsouzian, L.K., Schnakenberg, S.L., and Zakian, V.A. (2003). The Saccharomyces cerevisiae helicase Rrm3p facilitates replication past nonhistone protein-DNA complexes. Mol. Cell *12*, 1525–1536.

Jamonnak, N., Creamer, T.J., Darby, M.M., Schaughency, P., Wheelan, S.J., and Corden, J.L. (2011). Yeast Nrd1, Nab3, and Sen1 transcriptome-wide binding maps suggest multiple roles in post-transcriptional RNA processing. RNA *17*, 2011–2025.

Katou, Y., Kanoh, Y., Bando, M., Noguchi, H., Tanaka, H., Ashikari, T., Sugimoto, K., and Shirahige, K. (2003). S-phase checkpoint proteins Tof1 and Mrc1 form a stable replication-pausing complex. Nature *424*, 1078–1083.

Kerrest, A., Anand, R.P., Sundararajan, R., Bermejo, R., Liberi, G., Dujon, B., Freudenreich, C.H., and Richard, G.F. (2009). SRS2 and SGS1 prevent chromosomal breaks and stabilize triplet repeats by restraining recombination. Nat. Struct. Mol. Biol. *16*, 159–167.

Kim, H.D., Choe, J., and Seo, Y.S. (1999). The sen1(+) gene of Schizosaccharomyces pombe, a homologue of budding yeast SEN1, encodes an RNA and DNA helicase. Biochemistry *38*, 14697–14710.

Kogoma, T. (1997). Stable DNA replication: interplay between DNA replication, homologous recombination, and transcription. Microbiol. Mol. Biol. Rev. *61*, 212–238.

Köhler, A., and Hurt, E. (2007). Exporting RNA from the nucleus to the cytoplasm. Nat. Rev. Mol. Cell Biol. *8*, 761–773.

Koster, D.A., Crut, A., Shuman, S., Bjornsti, M.A., and Dekker, N.H. (2010). Cellular strategies for regulating DNA supercoiling: a single-molecule perspective. Cell *142*, 519–530.

Lengronne, A., McIntyre, J., Katou, Y., Kanoh, Y., Hopfner, K.P., Shirahige, K., and Uhlmann, F. (2006). Establishment of sister chromatid cohesion at the S. cerevisiae replication fork. Mol. Cell *23*, 787–799.

Li, X., and Manley, J.L. (2005). Inactivation of the SR protein splicing factor ASF/SF2 results in genomic instability. Cell *122*, 365–378.

Liberi, G., Maffioletti, G., Lucca, C., Chiolo, I., Baryshnikova, A., Cotta-Ramusino, C., Lopes, M., Pellicioli, A., Haber, J.E., and Foiani, M. (2005). Rad51-dependent DNA structures accumulate at damaged replication forks in sgs1 mutants defective in the yeast ortholog of BLM RecQ helicase. Genes Dev. *19*, 339–350.

Liberi, G., Cotta-Ramusino, C., Lopes, M., Sogo, J., Conti, C., Bensimon, A., and Foiani, M. (2006). Methods to study replication fork collapse in budding yeast. Methods Enzymol. *409*, 442–462.

Liu, L.F., and Wang, J.C. (1987). Supercoiling of the DNA template during transcription. Proc. Natl. Acad. Sci. USA *84*, 7024–7027.

Mirkin, E.V., and Mirkin, S.M. (2007). Replication fork stalling at natural impediments. Microbiol. Mol. Biol. Rev. *71*, 13–35.

Mischo, H.E., Gómez-González, B., Grzechnik, P., Rondón, A.G., Wei, W., Steinmetz, L., Aguilera, A., and Proudfoot, N.J. (2011). Yeast Sen1 helicase protects the genome from transcription-associated instability. Mol. Cell *41*, 21–32.

Moreira, M.C., Klur, S., Watanabe, M., Németh, A.H., Le Ber, I., Moniz, J.C., Tranchant, C., Aubourg, P., Tazir, M., Schöls, L., et al. (2004). Senataxin, the ortholog of a yeast RNA helicase, is mutant in ataxia-ocular apraxia 2. Nat. Genet. *36*, 225–227.

Nonet, M., Scafe, C., Sexton, J., and Young, R. (1987). Eucaryotic RNA polymerase conditional mutant that rapidly ceases mRNA synthesis. Mol. Cell. Biol. *7*, 1602–1611.

Nudler, E. (2012). RNA polymerase backtracking in gene regulation and genome instability. Cell *149*, 1438–1445.

Olavarrieta, L., Martínez-Robles, M.L., Hernández, P., Krimer, D.B., and Schvartzman, J.B. (2002). Knotting dynamics during DNA replication. Mol. Microbiol. *46*, 699–707.

Page, B.D., and Snyder, M. (1992). CIK1: a developmentally regulated spindle pole body-associated protein important for microtubule functions in Saccharomyces cerevisiae. Genes Dev. *6*, 1414–1429.

Pagès, V., and Fuchs, R.P. (2003). Uncoupling of leading- and lagging-strand DNA replication during lesion bypass in vivo. Science *300*, 1300–1303.

Papouli, E., Chen, S., Davies, A.A., Huttner, D., Krejci, L., Sung, P., and Ulrich, H.D. (2005). Crosstalk between SUMO and ubiquitin on PCNA is mediated by recruitment of the helicase Srs2p. Mol. Cell *19*, 123–133.

Paulsen, R.D., Soni, D.V., Wollman, R., Hahn, A.T., Yee, M.C., Guan, A., Hesley, J.A., Miller, S.C., Cromwell, E.F., Solow-Cordero, D.E., et al. (2009). A genome-wide siRNA screen reveals diverse cellular processes and pathways that mediate genome stability. Mol. Cell *35*, 228–239.

Pomerantz, R.T., and O'Donnell, M. (2008). The replisome uses mRNA as a primer after colliding with RNA polymerase. Nature *456*, 762–766.

Postow, L., Ullsperger, C., Keller, R.W., Bustamante, C., Vologodskii, A.V., and Cozzarelli, N.R. (2001). Positive torsional strain causes the formation of a four-way junction at replication forks. J. Biol. Chem. *276*, 2790–2796.

Rasmussen, T.P., and Culbertson, M.R. (1998). The putative nucleic acid helicase Sen1p is required for formation and stability of termini and for maximal rates of synthesis and levels of accumulation of small nucleolar RNAs in Saccharomyces cerevisiae. Mol. Cell. Biol. *18*, 6885–6896.

Rocha, E.P. (2008). The organization of the bacterial genome. Annu. Rev. Genet. *42*, 211–233.

Rondón, A.G., Mischo, H.E., Kawauchi, J., and Proudfoot, N.J. (2009). Fail-safe transcriptional termination for protein-coding genes in S. cerevisiae. Mol. Cell *36*, 88–98.

Rudolph, C.J., Dhillon, P., Moore, T., and Lloyd, R.G. (2007). Avoiding and resolving conflicts between DNA replication and transcription. DNA Repair (Amst.) *6*, 981–993.

Sabouri, N., McDonald, K.R., Webb, C.J., Cristea, I.M., and Zakian, V.A. (2012). DNA replication through hard-to-replicate sites, including both highly transcribed RNA Pol II and Pol III genes, requires the S. pombe Pfh1 helicase. Genes Dev. *26*, 581–593.

Shirahige, K., Iwasaki, T., Rashid, M.B., Ogasawara, N., and Yoshikawa, H. (1993). Location and characterization of autonomously replicating sequences from chromosome VI of Saccharomyces cerevisiae. Mol. Cell. Biol. *13*, 5043–5056.

Skourti-Stathaki, K., Proudfoot, N.J., and Gromak, N. (2011). Human senataxin resolves RNA/DNA hybrids formed at transcriptional pause sites to promote Xrn2-dependent termination. Mol. Cell *42*, 794–805.

Spencer, F., Gerring, S.L., Connelly, C., and Hieter, P. (1990). Mitotic chromosome transmission fidelity mutants in Saccharomyces cerevisiae. Genetics *124*, 237–249.

Steinacher, R., Osman, F., Dalgaard, J.Z., Lorenz, A., and Whitby, M.C. (2012). The DNA helicase Pfh1 promotes fork merging at replication termination sites to ensure genome stability. Genes Dev. *26*, 594–602.

Steinmetz, E.J., Conrad, N.K., Brow, D.A., and Corden, J.L. (2001). RNA-binding protein Nrd1 directs poly(A)-independent 3′-end formation of RNA polymerase II transcripts. Nature *413*, 327–331.

Stirling, P.C., Chan, Y.A., Minaker, S.W., Aristizabal, M.J., Barrett, I., Sipahimalani, P., Kobor, M.S., and Hieter, P. (2012). R-loop-mediated genome instability in mRNA cleavage and polyadenylation mutants. Genes Dev. *26*, 163–175.

Suraweera, A., Becherel, O.J., Chen, P., Rundle, N., Woods, R., Nakamura, J., Gatei, M., Criscuolo, C., Filla, A., Chessa, L., et al. (2007). Senataxin, defective in ataxia oculomotor apraxia type 2, is involved in the defense against oxidative DNA damage. J. Cell Biol. *177*, 969–979.

Suraweera, A., Lim, Y., Woods, R., Birrell, G.W., Nasim, T., Becherel, O.J., and Lavin, M.F. (2009). Functional role for senataxin, defective in ataxia oculomotor apraxia type 2, in transcriptional regulation. Hum. Mol. Genet. *18*, 3384–3396.

Thiebaut, M., Kisseleva-Romanova, E., Rougemaille, M., Boulay, J., and Libri, D. (2006). Transcription termination and nuclear degradation of cryptic unstable transcripts: a role for the nrd1-nab3 pathway in genome surveillance. Mol. Cell *23*, 853–864.

Tuduri, S., Crabbé, L., Conti, C., Tourrière, H., Holtgreve-Grez, H., Jauch, A., Pantesco, V., De Vos, J., Thomas, A., Theillet, C., et al. (2009). Topoisomerase I suppresses genomic instability by preventing interference between replication and transcription. Nat. Cell Biol. *11*, 1315–1324.

Ursic, D., Himmel, K.L., Gurley, K.A., Webb, F., and Culbertson, M.R. (1997). The yeast SEN1 gene is required for the processing of diverse RNA classes. Nucleic Acids Res. *25*, 4778–4785.

Vasiljeva, L., and Buratowski, S. (2006). Nrd1 interacts with the nuclear exosome for 3′ processing of RNA polymerase II transcripts. Mol. Cell *21*, 239–248.

Vizeacoumar, F.J., van Dyk, N., S Vizeacoumar, F., Cheung, V., Li, J., Sydorskyy, Y., Case, N., Li, Z., Datti, A., Nislow, C., et al. (2010). Integrating high-throughput genetic interaction mapping and high-content screening to explore yeast spindle morphogenesis. J. Cell Biol. *188*, 69–81.

Wahba, L., Amon, J.D., Koshland, D., and Vuica-Ross, M. (2011). RNase H and multiple RNA biogenesis factors cooperate to prevent RNA:DNA hybrids from generating genome instability. Mol. Cell *44*, 978–988.

Wang, J.C. (2002). Cellular roles of DNA topoisomerases: a molecular perspective. Nat. Rev. Mol. Cell Biol. *3*, 430–440.

Weinert, T.A., and Hartwell, L.H. (1988). The RAD9 gene controls the cell cycle response to DNA damage in Saccharomyces cerevisiae. Science *241*, 317–322.

Wlotzka, W., Kudla, G., Granneman, S., and Tollervey, D. (2011). The nuclear RNA polymerase II surveillance system targets polymerase III transcripts. EMBO J. *30*, 1790–1803.

Xu, H., Boone, C., and Klein, H.L. (2004). Mrc1 is required for sister chromatid cohesion to aid in recombination repair of spontaneous damage. Mol. Cell. Biol. *24*, 7082–7090.

Yurov, Y.B., Vorsanova, S.G., and Iourov, I.Y. (2011). The DNA replication stress hypothesis of Alzheimer's disease. ScientificWorldJournal *11*, 2602–2612.